

# Visual and 3D Mapping for Steel Bridge Inspection Using a Climbing Robot

<sup>1</sup>Nhan H. Pham, <sup>1</sup>Hung M. La\*, <sup>2</sup>Quang P. Ha, <sup>3</sup>Sy N. Dang, <sup>3</sup>Anh H. Vo, <sup>3</sup>Quang H. Dinh

<sup>1</sup>Department of Computer Science and Engineering, University of Nevada, Reno, USA

<sup>2</sup>Faculty of Engineering and IT, University of Technology, Sydney, Australia

<sup>3</sup>Robotics Center, Duy Tan University, Da Nang, Vietnam

\*Corresponding Author: [hla@unr.edu](mailto:hla@unr.edu)

## Abstract –

There are over six hundred thousand bridges in the U.S. which require great amount of human effort along with expensive and specialized equipment for maintenance. Current bridge inspections are manually performed by inspectors which are inefficient and unsafe. This paper presents visual and three dimensional (3D) structure inspection for steel bridges and steel structures using the developed climbing robot. The robot can move freely on steel surface, carry several sensors, and collect data then send to the ground station for real-time monitoring as well as further processing. Steel surface image stitching and 3D map building are conducted to provide a current condition of the structure.

## Keywords –

Field robotics; Climbing robots; Steel bridge inspection.

## 1 Introduction

There are currently over six hundred thousand bridges in the U.S. [1] and twenty percent of them are steel bridges. Among those, more than fifty thousand bridges are either deficient or functionally obsolete which are likely a growing threat to human's safety. Collapse of numerous bridges recorded over past 15 years has shown significant impact on the safety of all travellers. For instance, the Minneapolis I-35W Bridge in Minnesota, collapsed in 2007 due to undersized gusset plates, increased concrete surfacing load, and weight of construction supplies/equipment [2]. The accident along with others have grown a demand of frequent and adequate bridge inspection and maintenance. However, current activities require great amount of human effort along with expensive and specialized equipment. Besides, most bridges inspections are manually inspected by human inspectors with visual inspection or hammer

tapping and chain dragging for delamination and corrosion detection which are very time consuming. Moreover, it is difficult and dangerous for the inspectors to climb up or hang on cables inspecting large bridges with high structures as shown in Figure 1. In addition, reports from visual inspection may vary among inspectors, hence the bridge's condition cannot be assessed precisely. Therefore, there should be a solution which provides consistent and accurate bridge condition report with high efficiency along with safety assurance. If a robot carrying several advanced evaluation sensors is able to climb on those bridges to collect data for condition assessment, it will significantly improve the inspection efficiency as well as enhance inspectors' safety since they no longer have to work under dangerous conditions.

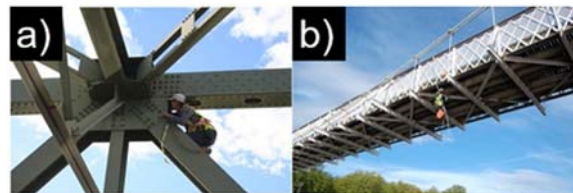


Figure 1. Dangerous bridge inspection (source: icaeng.com, hireuavpro.com).

The number of studies related to utilizing advanced technology for bridge inspection and evaluation has significant increased recently. In one hand, R.S Lim et al. [3], N. Gucunski et al. [4], and H.M. La et al. [5] introduce a novel robotic systems for bridge deck inspection, while the NDE technology and NDE data processing for bridge deck inspection and evaluation are presented in [6] and [7]. In [8] and [9], an autonomous robotic system integrated with advanced non-destructive evaluation (NDE) sensors for high-efficiency bridge deck inspection and evaluation. B. Li et al. [10] also utilized NDE technique to perform automatic inspection on

bridge deck and record bridge's health condition. In the other hand, there are several works focusing on cable inspection. F. Xu et al. [11] introduced the design and experiments of a wheel-based cable inspection robotic system consisting of CCD cameras for visual inspection. Similar robot from K.H. Cho et al. [12] enables effective visual inspection of the cable on suspension bridge. Besides, there were several initial implementations of climbing robots for bridge inspection including steel bridges. A. Mazumdar et al. [13] proposed a legged robot that moves across a steel structure for steel bridge inspection. Powerful permanent magnets embedded in each foot allow the robot to hang from a steel ceiling powerlessly while the attractive force is modulated by tilting the foot against the steel surface. A robot with magnetic wheels was developed by R. Wang, et al. [14] carrying Giant Magneto Resistive sensor array for crack and corrosion detection. Q. Liu et al. [15] and Y. Liu et al. [16] also proposed a bridge inspection method using a wall-climbing robot based on negative pressure adhesion mechanism which collects crack images with a high-resolution camera so that the crack can be extracted and analysed precisely. Based on attraction force created by permanent magnets, A. Leibbrandt et al. [17] and H. Leon-Rodriguez et al. [18] developed different wall-climbing robots carrying NDE devices to detect weld defects, cracks, corrosion testing that is capable of inspecting oil tanks or steel bridges. A. San-Millan [19] presented the development of a teleoperated wall climbing robot which can be equipped with various testing probes and cameras for different inspection tasks. D. Zhu et al. [20] used a magnetic wall-climbing robot capable of navigating on steel structures, measuring structural vibrations, processing measurement data and wirelessly communicating information to investigate field performance of flexure-based mobile sensing nodes and identify minor structural damage, and illustrate a high sensitivity in damage detection.

In this paper, the inspection technique using visual and three dimensional (3D) images integrated on our developed climbing robot [21] is introduced. The robot is able to strongly adhere and freely move on steel surface to collect images from visual camera as well as 3D camera. The captured images from visual camera are then stitched together to provide a whole image of steel surface that has been inspected. Moreover, a 3D map can be built from 3D data in order to assist robot navigation as well as inspecting bridge structures. With an advanced mechanical design, the robot is able to carry a heavy load (approximately 15 pounds) while climbing on both inclination and upside-down surfaces. The robot can also transit from one surface to another surface with up to 90 degrees change in orientation. Collected data are sent to a ground station in real time for further processing. Steel surface image stitching and 3D structure map are

generated from collected data to provide a condition of the bridges.

The rest of this paper is organized as follows. Section 2 describes the overall robot design. Section 3 presents data collection and processing. Section 4 shows various experiments to verify robot design and data processing. Finally, Section 5 gives the conclusion and future work.

## 2 Overall Design

### 2.1 Mechanical Design

A four motorized wheels robot design as shown in Figure 2 is proposed which takes advantage of permanent magnets for adhesion force creation. Therefore, it allows the robot to adhere to steel surfaces without consuming any power. In addition, cylinder shaped magnets are used for convenience and flexibility in adjusting the attraction force. Moreover, eight high torque servo motors (525g/mm) are modified to use for driving four wheels and four shafts – which are used for robot lifting to avoid being stuck in rough terrain.

36 Neodymium magnet cylinders embedded in each wheel can create magnetic force up to 14 kg/wheel if there is no air gap between the magnets and the steel surface [21]. However, each wheel is covered by a thin layer of cloth to enhance the friction with steel surface, hence the magnetic force created is reduced which is approximately 6 kg/wheel. Additionally, a mechanism has been added in order to lift either front or rear wheels off if the robot is stuck on rough terrains.

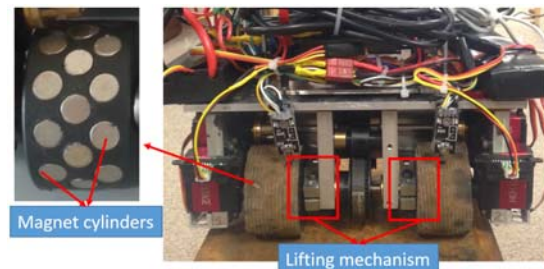


Figure 2. Embedded magnet cylinders and lifting mechanism.

When moving on steel surfaces, there are problems needed to be addressed in order to maintain stability of the robot which are sliding and turn-over failure. Our previous work [21] shows that in order to avoid two types of failure, the magnetic force created by all wheels should satisfy

$$F_{mag} > \max \left\{ 2.237P; 2 \frac{Pd}{L} \right\}, \quad (1)$$

where  $F_{mag}$  is the total magnetic force,  $P$  is the robot's weight ( $P = mg$  where  $m$  is robot's mass and  $g$  is gravitational acceleration),  $d$  is the distance between the center of mass to steel surface, and  $L$  is the distance between front and rear wheels.

## 2.2 System Integration

Overall, the structure of the system is shown in Figure 3 and the robot with fully installed sensors and other components are depicted in Figure 4.

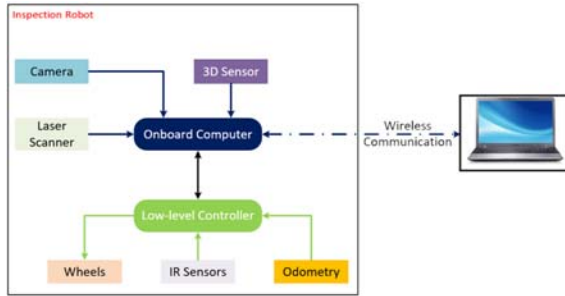


Figure 3. System architecture.

Regarding sensing devices, the robot is equipped with multiple imaging sensors: two video cameras for images capturing and video streaming, and a time-of-flight (ToF) camera for capturing 3D data. The USB camera in the back of the robot is installed facing downward to the steel surface in order to take images of steel surfaces to feed the image stitching technique. Besides, the ToF camera is placed so that 3D images received from the camera can assist navigation as well as 3D structure construction.

Apart from cameras, eight Hall Effect sensors which are able to detect the presence of magnetic field are also used. We use two sensors which are mounted next to each other and close to robot's wheel. By taking advantage of

the fact that magnet cylinders inside each wheel will move when the robot moves, we can extract the velocity and traveling distance of each wheel after combining the data from these two sensors.

Besides, the robot has four IR range sensors mounted at four corners of the robot, which can detect whether there exists a surface underneath. Consequently, an edge avoidance algorithm can be implemented using this input to make sure that the robot can safely travel on steel surfaces.

The robot is controlled by two controllers: a microcontroller (MCU) based controller handling low-level tasks, and a powerful on-board computer for complex processing and communication with ground station. The low-level controller has the capability of receiving commands from on-board computer via serial connection including motion control, sensors data acquisition. The on-board computer is a NUC Core i3 computer from Intel which captures video camera frames and 3D camera images then sends them to ground station over wireless LAN connection for data post processing and logging. It also executes the edge avoidance algorithm with sensors data received from the low-level controller to ensure safe traveling on steel surfaces.

## 2.3 Robot Navigation

While moving on steel surfaces, there can be a circumstance that the robot moves far away toward the edge of the surface which may cause it to fall off. Therefore, an algorithm using input from IR range sensors is incorporated to prevent this failure. Denote  $r_{cal_i}$  ( $i = 1, \dots, 4$  is the index of four IR sensors of the robot) as the calibrated ranges before robot starts moving,  $r_i$  ( $i = 1, \dots, 4$ ) as IR sensor reading corresponding to  $sensor_i$  and  $d_i$  ( $i = 1, \dots, 4$ ) as travel distances calculated from Hall Effect sensors. When sensor reading is out of the range between  $[r_{cal_i} - \varepsilon; r_{cal_i} + \varepsilon]$  where  $\varepsilon$  is a predefined threshold, the robot considers that there is no surface below  $sensor_i$ .

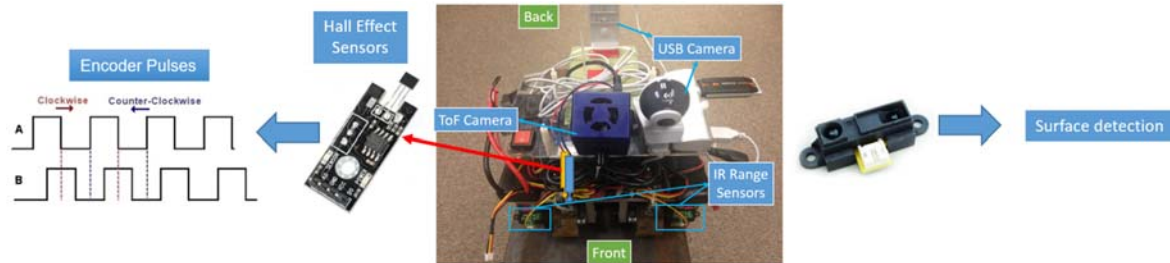


Figure 4. Robot prototype with integrated sensors.

---

**Algorithm 1:** Edge Avoidance.
 

---

**Input:**  $(r_{cal_1}, r_{cal_2}, r_{cal_3}, r_{cal_4}), (r_1, r_2, r_3, r_4), \varepsilon, (d_1, d_2, d_3, d_4)$

1. **for**  $i=1:4$  **do**
  2.     **if** only one  $(r_i) \notin [r_{cal_i} - \varepsilon; r_{cal_i} + \varepsilon]$  **then**
  3.         **if**  $i = \text{front right IR sensor}$  **then**
  4.             Stop
  5.             Go backward with a distance of 5 cm ( $\Delta d_i \approx 3$ ).
  6.             Rotate left when travel distance of either right wheels reach 3 cm ( $\Delta r_i \approx 2$ ).
  7.             Keep moving.
  8.             Check other sensors and take similar actions.
  9.     **else stop and wait for commands.**
- 

Moreover, the velocity and distance calculated from Hall Effect sensor reading can help implement the automatic images capturing so that we can stitch all collected images to detect corrosion or defect on steel surface. In this mode, the robot need to stop after traveling a particular distance to ensure that the two consecutive images are overlapped.

### 3 Data Collection and Processing

#### 3.1 Image Stitching

In order to enhance steel surface inspection, we combine image sequences. Captured images are saved to the memory so that they can be processed later when the robot finished its operation.

In this technique, it is required that two consecutively taken images are at least 30% overlapped as shown in Figure 5. The camera can cover an area of 18cm x 14cm which means the robot should stop and capture images every 12 cm.

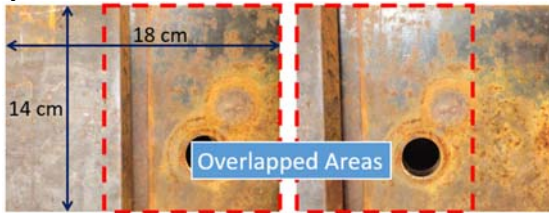


Figure 5. Overlapped images used for stitching.

While stitching all of the images, we can also transform the stitched image's coordinate to the world's coordinate. Denote  $(X_{im}, Y_{im}, Z_{im})$  as the coordinates of image frame,  $(X_{cam}, Y_{cam}, Z_{cam})$  are coordinates of camera frame,  $(X_r, Y_r, Z_r)$  are coordinates of robot frame

and  $(X_w, Y_w, Z_w)$  are coordinates of the world fix frame as shown in Figure 6.

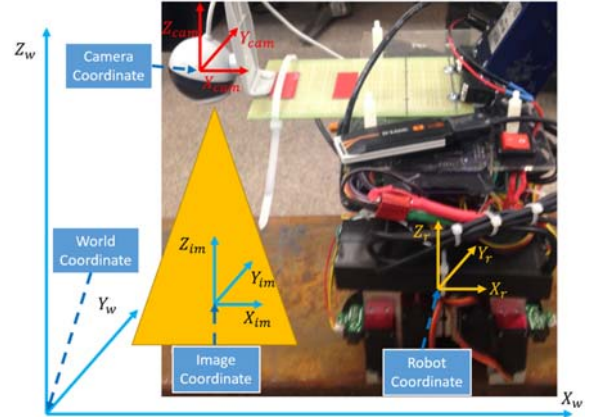


Figure 6. Relationship between multiple frames.

The following series of transformation should be done to convert coordinates in image frame to world frame:

$$\begin{aligned} (X_{im}, Y_{im}, Z_{im}) &\xrightarrow{T_{ic}} (X_{cam}, Y_{cam}, Z_{cam}) \\ &\quad \downarrow \vec{q} \\ (X_w, Y_w, Z_w) &\xleftarrow{T_{rw}} (X_r, Y_r, Z_r) \end{aligned}$$

where  $T_{ij}$  are the transform matrix from frame  $i$  to frame  $j$ . Since the camera mounting location is fixed on the robot,  $T_{ic}$  and  $T_{cr}$  can be easily calculated by measuring the distance between the camera and the steel surface and the robot's centre of mass while  $T_{rw}$  can be extracted from odometry. For more details of this transformation, please refer to [23].

#### 3.2 3D Construction

The concept of 3D construction or 3D registration is based on the Iterative Closest Point (ICP) algorithm introduced by Besl et al. [24] and Y. Chen [25] in the early 1990s. The algorithm was used to construct 3D model of objects and has later been employed for robotic applications including 2D, 3D mapping and localization [26]. The goal of the ICP is to find the transformation parameters (rotation and translation) that align an input point cloud to a reference point cloud. Those transformation parameters are presented in the coordinate frame of the reference point cloud. Figure 7 shows the process of 3D registration including ICP algorithm consisting of following steps [26], [27]:

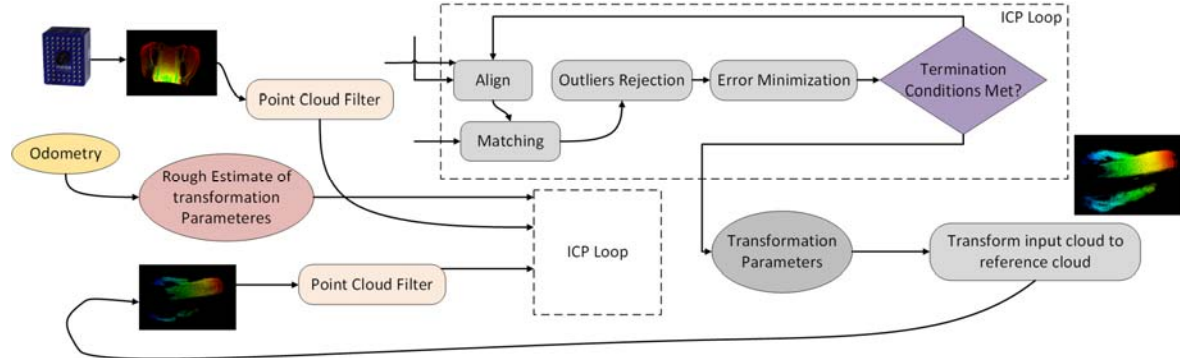


Figure 7. 3D map construction process employing ICP algorithm.

1. Selection: Input point cloud captured from ToF camera are pre-sampling for higher efficiency.
2. Matching: Odometry data can be used to estimate the correspondences between the points in the subsampled point clouds considered as the initial alignment.
3. Rejection: Filtering the correspondences to reduce the number of outliers, multiple points with same corresponding point are rejected.
4. Alignment: Calculating assessment criteria which are normally point-to-point or point-to-plane error metrics, then minimizing it to find the optimal transformation.

The algorithm stops when one of these case happens:

1. Convergence: the error metric falls under a threshold or remain constant; or the transformation parameters become unchanged.
2. The algorithm does not converge after a given number of iterations.
3. Transformation parameters are out of bound.

#### 4 Experimental Results

In order to verify the edge avoidance algorithm as well as the data collection and processing technique, we have conducted multiple experiments under lab environment utilizing different steel bars. During the test, one 2S1P (2 cells) 7.4V 5000 milliampere-hour (mAh) and one 3S1P 11.1V 5000 mAh batteries are used to power the robot. One laptop which can connect to a wireless LAN is used as a ground station.

First of all, the full robot with all sensor integrated is tested to climb on a vertical steel surface in order to verify the load carrying capability. During the test, the robot strongly adheres to steel structure as shown in Figure 8. Another test is conducted when robot moves on a constructed steel structures from one end to the other end as depicted in Figure 9. The robot successfully reaches

the destination as well as using lifting mechanism to overcome stuck condition as shown in Figure 9.b.



Figure 8. Robot moves on vertical surface while carrying all sensors.

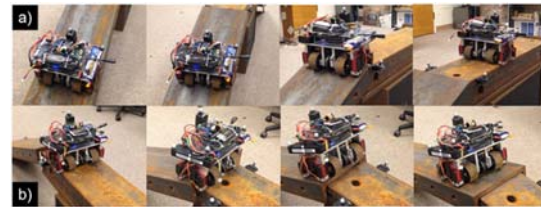


Figure 9. Robot moves on a bridge-like steel structure with Edge Avoidance.

During the test, data collected from both video camera and depth camera are transmitted over wireless connection to the laptop acting as ground station. Received data are illustrated in Figure 10.

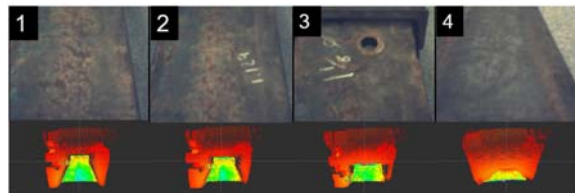


Figure 10. Visual and depth images from cameras showing the condition of the bridge surface. Top images show visual condition, and bottom images show the 3D structure maps.

Regarding 3D construction capability, the robot moves on a flat steel structure as shown in Figure 11. While the robot is traveling on the structure, 3D images are captured from the ToF camera. The data is both transferred to the ground station and saved to the on-board computer's hard disk. The 3D images are taken every 100 milliseconds in order to obtain enough overlapped area between two consecutive images. After the robot successfully reach the other end of the steel structure, we apply ICP algorithm to align all stored 3D images to form a 3D map of the environment including the steel structure. The 3D construction results are presented in Figure 12 and Figure 13.



Figure 11. Robot setup to test 3D construction capability.

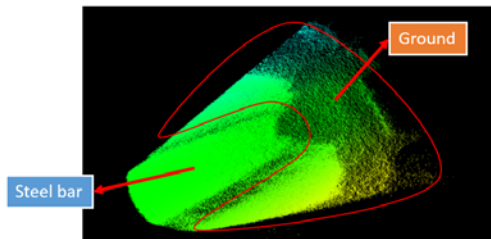


Figure 12. Resulting map from 3D images.

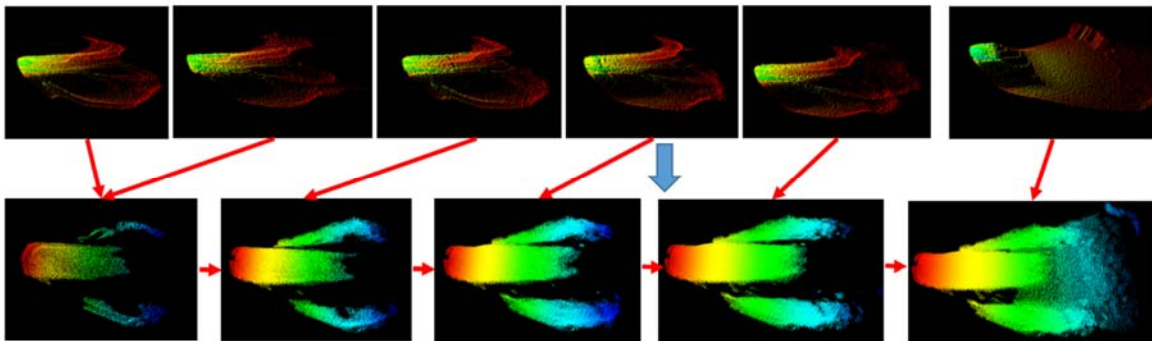


Figure 13. 3D registration from point cloud data.

Furthermore, from the images collected through the camera facing downward to the surface, we are able to stitch the images together. From the stitched image, we can spot some areas of steel structure which have been greatly or slightly deteriorated as shown in Figure 14.

## 5 Conclusion and Future Work

This work describes the visual and 3D structure inspection for steel bridges and steel structures using the developed climbing robot. The robot is able to carry several sensors and move safely on steel surfaces to collect data. The acquired visual and 3D images are transferred to ground station for real-time monitoring and processing. An image stitching technique has been implemented to create an entire image of steel surface from captured images. Moreover, various sensors are integrated to ensure safe navigation on steel surfaces.

Further work needed to be done including localization using combined odometry and camera data, implementation of map construction method as well as visual crack detection algorithm from stitched images. Additionally, a cooperative process can be used to employ multiple robots for faster inspecting a steel large bridge.

## Acknowledgments

This work is supported by the University of Nevada, Reno and the National Science Foundation under the grant: NSF-ICorps#1559942. The authors gratefully acknowledge contributions of: Luan Nguyen, Jesus Sanchez, and Tuan Le during the implementation and test of the robot at the Advanced Robotics and Automation (ARA) Lab.

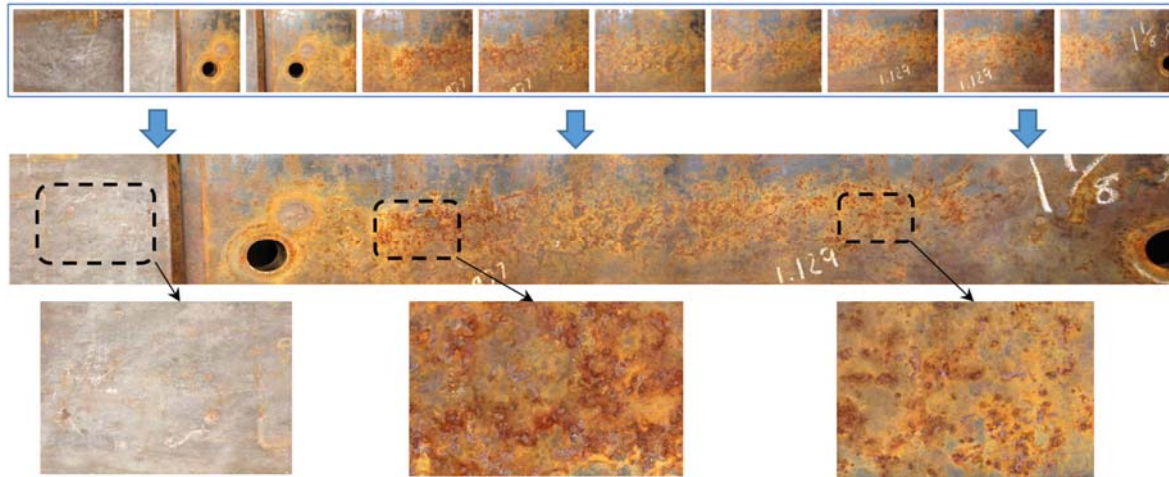


Figure 14. Images stitching result: (Top) 10 individual images taken by the robot; (Middle) Stitching image result from those 10 individual images; (Bottom) Closer look (zoom-in) at some areas, from left-to-right, showing “good condition”, “serious deteriorated condition”, and “light deteriorated condition” of the steel surface, respectively.

## References

- [1] U.S. Department of Transportation Federal Highway Administration. National Bridge Inventory Data. On-line: <http://www.fhwa.dot.gov/bridge/nbi.cfm>. Access: 01/30/2016.
- [2] I-35W St. Anthony Falls Bridge collapse. Minnesota Department of Transportation. On-line: <http://www.dot.state.mn.us/i35wbridge/collapse.html>. Access: 01/30/2016.
- [3] R.S. Lim, H.M. La and W. Sheng. A robotic crack inspection and mapping system for bridge deck maintenance. *IEEE Transactions on Automation Science and Engineering*, 11(2):367–378, April 2014.
- [4] N. Gucunski, S.H. Kee, H.M. La, B. Basily and A. Maher. Delamination and concrete quality assessment of concrete bridge decks using a fully autonomous RABIT platform. *International Journal of Structural Monitoring and Maintenance*, 2(1):19–34, 2015.
- [5] H.M. La, N. Gucunski, S.H. Kee, J. Yi, T. Senlet and L. Nguyen. Autonomous Robotic System for Bridge Deck Data Collection and Analysis. In *IEEE International Conference on Intelligent Robots and Systems (IROS)*, pages 1950–1955, Chicago, USA, 2014.
- [6] H.M. La, N. Gucunski, S.H. Kee, and L. Nguyen. Visual and Acoustic Data Analysis for the Bridge Deck Inspection Robotic System. In *31st International Symposium on Automation and Robotics in Construction and Mining (ISARC)*, pages 50–57, Sydney, Australia, 2014.
- [7] N. Gucunski, B. Basily, S.H. Kee, H.M. La, H. Pavardeh, A. Maher and H. Gashemi. Multi NDE Technology Condition Assessment of Concrete Bridge Decks by RABITTM Platform. In *NDE/NDT for Structural Materials Technology for Highway & Bridges*, August 25, 2014.
- [8] H.M. La, R.S. Lim, B.B. Basily, N. Gucunski, J. Yi, A. Maher, F.A. Romero, and H. Parvardeh. Mechatronic systems design for an autonomous robotic system for high-efficiency bridge deck inspection and evaluation. *IEEE/ASME Transactions on Mechatronics*, 18(6):1655–1664, Dec 2013.
- [9] H.M. La, N. Gucunski, S.H. Kee, and L.V. Nguyen. Data analysis and visualization for the bridge deck inspection and evaluation robotic system. *Visualization in Engineering*, 3(1):1–16, 2015.
- [10] B. Li, J. Cao, J. Xiao, X. Zhang, and H. Wang. Robotic Impact-Echo Non-Destructive Evaluation Based On FFT and SVM. In *2014 11th World Congress on Intelligent Control and Automation (WCICA)*, pages 2854–2859, Shenyang, China, 2014.
- [11] F. Xu, and X. Wang. Design and Experiments on a New Wheel-Based Cable Climbing Robot. In *IEEE/ASME International Conference on Advanced Intelligent Mechatronics (AIM)*, pages 418–423, Xian, China, 2008.
- [12] K.H. Cho, H.M. Kim, Y.H. Jin, F. Liu, H. Moon, J.C. Koo, and H.R. Choi. Inspection robot for hanger cable of suspension bridge: Mechanism Design and Analysis. *IEEE/ASME Transactions on Mechatronics*, 18(6):1665–1674, Dec 2013.

- [13] A. Mazumdar, and H.H. Asada. Mag-Foot: A Steel Bridge Inspection Robot. In *IEEE/RSJ International Conference on Intelligent Robots and Systems (IROS)*, pages 1691–1696, Missouri, USA, 2009.
- [14] R. Wang, and Y. Kawamura. A Magnetic Climbing Robot for Steel Bridge Inspection. In *2014 11th World Congress on Intelligent Control and Automation (WCICA)*, pages 3303–3308, Shenyang, China, June 2014.
- [15] Q. Liu, and Y. Liu. An Approach for Auto Bridge Inspection Based On Climbing Robot. In *2013 IEEE International Conference on Robotics and Biomimetics (ROBIO)*, pages 2581–2586, Shenzhen, China, Dec 2013.
- [16] Y. Liu, Q. Dai, and Q. Liu. Adhesion-Adaptive Control of a Novel Bridge-Climbing Robot. In *2013 IEEE 3rd Annual International Conference on Cyber Technology in Automation, Control and Intelligent Systems (CYBER)*, pages 102–107, Nanjing, China, May 2013.
- [17] A. Leibbrandt, G. Caprari, U. Angst, R.Y. Siegwart, R.J. Flatt, and B. Elsener. Climbing Robot for Corrosion Monitoring of Reinforced Concrete Structures. In *2012 2nd International Conference on Applied Robotics for the Power Industry (CARPI)*, pages 10–15, Zurich, Switzerland, Sept 2012.
- [18] H. Leon-Rodriguez, S. Hussain, and T. Sattar. A Compact Wall-Climbing and Surface Adaptation Robot for Non-Destructive Testing. In *2012 12th International Conference on Control, Automation and Systems (ICCAS)*, pages 404–409, Korea, Oct 2012.
- [19] A. San-Millan. Design of a Teleoperated Wall Climbing Robot for Oil Tank Inspection. In *2015 23th Mediterranean Conference on Control and Automation (MED)*, pages 255–261, Torremolinos, Spain, June 2015.
- [20] D. Zhu, J. Guo, C. Cho, Y. Wang, and K.M. Lee. Wireless Mobile Sensor Network for the System Identification of a Space Frame Bridge. *IEEE/ASME Transactions on Mechatronics*, 17(3):499–507, June 2012.
- [21] N.H. Pham and H.M. La. Design and Implementation of an Autonomous Robot for Steel Bridge Inspection. Manuscript submitted to *2016 IEEE/RSJ International Conference on Intelligent Robots and Systems (IROS)*, 2016.
- [22] K&J Magnetics Inc. Original magnet calculator. On-line: <http://www.kjmagnetics.com>, Accessed: 01/30/2016.
- [23] R.S. Lim, H.M. La, Z. Shan and W. Sheng. Developing a crack inspection robot for bridge maintenance. In *IEEE International Conference on Robotics and Automation (ICRA)*, Shanghai, China, May, 2011.
- [24] P. Besl and N. McKay. A method for registration of 3-D shapes. *IEEE Transaction on Pattern Analysis and Machine Intelligence*, 14(2):239–256, 1992.
- [25] Y. Chen and G. Medioni. Object modelling by registration of multiple range images. In 1991 Proceedings of the IEEE International Conference on Robotics and Automation, 3:2724–2729, 1991.
- [26] T. Candia. ICP optimization for 3D robot mapping. Master Thesis, Swiss Federal Institute of Technology in Zurich, 2011.
- [27] D. Holz, A. E. Ichim, F. Tombari, R. B. Rusu and S. Behnke. Registration with the point cloud library: a modular framework for aligning in 3-D. *IEEE Robotics & Automation Magazine*, 2(4):110–124, Sept 2015